Somatic Mutation and Light Chain Rearrangement Generate Autoimmunity in Anti–single-stranded DNA Transgenic MRL/*lpr* Mice

By Frederic Brard,* Michele Shannon,* Eline Luning Prak,‡ Samuel Litwin,§ and Martin Weigert*

*From the *Department of Molecular Biology, Princeton University, Princeton, New Jersey 08544; the ‡Department of Pathology and Laboratory Medicine and the Department of Genetics, University of Pennsylvania School of Medicine, Philadelphia, Pennsylvania 19104; and the §Fox Chase Cancer Center, Institute for Cancer Research, Philadelphia, Pennsylvania 19111*

Summary

Antibodies to single-stranded (ss)DNA are expressed in patients with systemic lupus erythematosus and in lupus-prone mouse models such as the MRL/Mp-*lpr/lpr* (MRL/*lpr*) strain. In nonautoimmune mice, B cells bearing immunoglobulin site-directed transgenes (sd-tgs) that code for anti-ssDNA are functionally silenced. In MRL/*lpr* autoimmune mice, the same sd-tgs are expressed in peripheral B cells and these autoantibodies gain the ability to bind other autoantigens such as double-stranded DNA and cell nuclei. These new specificities arise by somatic mutation of the anti-ssDNA sd-tgs and by secondary light chain rearrangement. Thus, B cells that in normal mice are anergic can be activated in MRL/*lpr* mice, which can lead to the generation of pathologic autoantibodies. In this paper, we provide the first direct evidence for peripheral rearrangement in vivo.

Key words: anti-DNA • B cell tolerance • receptor editing • systemic lupus erythematosus • V_H replacement

The autoantibody specificities in SLE are biased toward DNA and nucleoproteins (1). These autoantibodies, known collectively as antinuclear antibodies (ANAs),[1] are diagnostic of SLE, but individuals with this disease express unique subsets of ANAs (2). The limited spectra of autoantibodies, both in the general population and among individuals with SLE, suggest that these autoantibodies arise by immunization (2). The oligoclonality of autoantibodies in SLE and other systemic autoimmune diseases of humans and mice confirms that autoantibodies arise by antigen activation (3, 4). The subsets of autoantibodies expressed by SLE patients are often directed to "physically-linked epitopes," for example, DNA and histones (5). Because it is unlikely that a pathogen would mimic multiple self-epitopes, autoantibodies to linked epitopes argue that the immunogens in SLE are complex structures, such as nucleosomes, made up of DNA and DNA binding proteins. Interestingly, complex antigens containing the common targets of SLE autoantibodies, such as DNA, Ro, and La, are found in blebs on the surface of dying cells (6). These blebs could be the delivery vehicles of self-antigen, especially in tissues undergoing extensive apoptosis.

That autoantibodies directed against ubiquitous self-antigens such as DNA resemble antibodies to foreign antigens implies that all individuals have the potential for generating these specificities. Hence, autoreactive B cells must be under active, negative regulation in nonautoimmune individuals. Mice with transgenes coding for autoantibodies have been useful tools for studying self-tolerance and have demonstrated that this is the case; B cells specific for facultative or constitutive self-antigens undergo receptor editing, become anergic, or, if all else fails, are deleted (7–14). The use of these models has been extended to the study of why self-tolerance fails in autoimmune disease, and autoantibody transgenes have been crossed to MRL/*lpr* and *lpr/lpr* congenic mice for this purpose (15–19). The *lpr* mutation inactivates the Fas receptor (CD95), thereby protecting Fas-sensitive cells from programmed cell death (for review see reference 20). Thus, the extent to which Fas-dependent apoptosis contributes to the regulation of autoreactive B cells is testable in these transgenic *lpr/lpr* mice.

The transgenes directed to the facultative self-antigens, hen egg lysozyme (HEL) and an MHC product, H-2K^k, have yielded unexpected results. Central tolerance to H-2K^k

[1]*Abbreviations used in this paper:* ANA, antinuclear antibody; dsDNA, double-stranded DNA; FW, framework; HEL, hen egg lysozyme; MRL/*lpr*, MRL/Mp-*lpr/lpr* mouse; RAG, recombination-activating gene; sd-tg, site-directed transgene; ssDNA, single-stranded DNA.

and the membrane form of HEL, which is achieved by elimination of the specificities for these antigens, appears to be intact in anti–H-2K and anti-HEL *lpr/lpr* mice (15, 17). Also, tolerance to the soluble forms of HEL and MHC was not broken in *lpr/lpr* mice (15, 16). However, in transgenic anti-DNA *lpr/lpr* mice, tolerance to DNA is broken (18). Hence, a selective breakdown of tolerance may explain the limited spectrum of autoantibodies seen in MRL/*lpr* or *lpr/lpr* congenics, a spectrum that includes anti-DNA but not anti-H2. Selective breakdown of tolerance could be explained by the affinity of the receptor for self-antigen, features of the self-antigen such as concentration, or by the chronology of antigen presentation. The previous study on anti-DNA transgenic *lpr/lpr* mice (18) was not informative in this regard because the level and time at which tolerance to DNA was broken could not be ascertained. Here we describe studies on an anti–single-stranded (ss)DNA transgenic *lpr/lpr* mouse in which the specificity of the anti-DNA is explicitly known (12, 21) and the mechanism of regulation in normal mice is understood in detail (13). Our studies show that anti-DNA expression in *lpr/lpr* mice is due to a combination of loss of peripheral tolerance (anergy) and inappropriate activation of defunct B cells.

Materials and Methods

Mice. The construction of site-directed transgenic (sd-tg) mice expressing the H and/or L chain genes coding for well-defined anti-DNA Abs has been described previously (22, 23). BALB/c 3H9Vκ8 sd-tg mice (3H9Vκ8/BALB/c) were crossed onto the MRL-*lpr/lpr* background and backcrossed three times to generate 3H9Vκ8 MRL-*lpr/lpr* mice (3H9Vκ8/*lpr*). Animals homozygous for the *lpr* gene were identified by two PCR assays using tail DNA. In brief, 1–2 mm of tail was snipped off and placed into 80 μl tail digestion buffer (50 mM Tris-HCl, pH 8.0, 50 mM KCl, 2.5 mM EDTA, 0.45% NP-40, and 0.45% Tween 20) containing 2 μl proteinase K (20 mg/ml; Boehringer Mannheim). After overnight incubation at 55°C, tail samples were boiled for 10 min and kept on ice. 1 μl of tail DNA was used for both PCR assays. The oligonucleotides used for these PCRs have been described previously (24). They were Fas-I2F (forward: 5′ agcatagattccatttgct 3′), with Fas-Z8 (reverse: 5′-caaattttattgttgcgaca-3′) to identify the *lpr* allele, or Fas-I2B (reverse: 5′-agtaatgggctcagtgca-3′) to identify the wild-type *fas* allele. PCR amplifications were set up in 50-μl vol containing 1 U of AmpliTaq Gold™ (Perkin Elmer Corp.), 1× buffer II, 250 μM of each dNTP, 2.5 mM $MgCl_2$, and 40 pmol of each primer. Amplifications were carried out in an OmniGene Hybaid thermocycler (Hybaid) under the following conditions: denaturation/enzyme activation for 9 min at 92°C; then 35 cycles of 30 s each at 94, 56, and 72°C; final elongation at 72°C for 7 min.

B Cell Hybridoma Production. B cell hybridomas were generated from unmanipulated spleen cells from a 2-mo-old 3H9Vκ8/*lpr* mouse using SP2/0 myeloma cells (25) as the fusion partner. Spleen cells from 3H9Vκ8/BALB/c mice were stimulated in vitro for 3 d with 20 μg/ml LPS (Sigma Chemical Co.) and fused as previously described (13). Hybridomas were plated at limiting dilution, and only wells bearing single colonies on 96-well plates containing <30 hybrids per plate were expanded for analysis.

ELISA Assay for Ig Secretion. Isotypes were determined using an indirect solid-phase ELISA as previously described (26). Plates were coated with anti-Ig Ab and developed with alkaline phosphatase–labeled anti-IgM, anti-IgG, anti-IgA, anti-κ, or anti-λ. The enzyme activity was revealed by the substrate *p*-nitrophenyl phosphate (Sigma Chemical Co.) and optical density was read at 405 nm. All commercial Abs were from Southern Biotechnology Associates, Inc. Samples were titrated, and concentrations were estimated by comparison to a standard curve.

DNA Binding Assays. Binding to ssDNA was measured by solid phase ELISA. Immunolon® 4 plates (Dynex Technologies, Inc.) were coated with 60 μl of histone-free protamine (Sigma Chemical Co.) at 500 μg/ml. Then, 60 μl of boiled and quickly chilled salmon sperm DNA (90 μg/ml) was allowed to bind to protamine-coated plates overnight at 4°C in a humid chamber. The next day, the plates were blocked with PBS containing 1% BSA. After washing with PBS-Tween, serum samples or hybridoma supernatants at various dilutions were added and incubated for 2 h at 37°C. To detect DNA binders, alkaline phosphatase–labeled mouse isotype-specific antibody was used (Southern Biotechnology Associates, Inc.), and the enzyme activity was revealed by the specific substrate *p*-nitrophenyl phosphate (Sigma Chemical Co.). Optical density was read at 405 nm.

Binding to dsDNA was measured by a two-step solution phase ELISA as previously described (27). In brief, antibody concentrations in the supernatants were first standardized to 2 μg/ml. Then, supernatants and protein-free calf thymus biotinylated DNA (1 μg/ml) were mixed, incubated at 37°C for 60 min, and transferred to microtiter plates (Immunolon® 4; Dynex Technologies, Inc.) coated with pure avidin (10 μg/ml, 50 μl/well; Avidin D; Vector Labs., Inc.). After a 60-min incubation at room temperature, plates were washed, and DNA–Ab complexes were detected with alkaline phosphatase–conjugated goat anti–mouse isotype-specific Ab (Southern Biotechnology Associates, Inc.).

Immunofluorescence (ANAs and Crithidia luciliae). Antinuclear specificities of mAbs and serum Igs were determined by indirect immunofluorescence staining of HEp-2 cells using an ANA test kit (The Binding Site, Inc.) according to the manufacturer's directions. Substrate cells were incubated with culture supernatants or serum at different dilutions for 20 min, washed in cold PBS/BSA 1%, and stained with Alexa™ 488 goat anti–mouse IgG (Molecular Probes, Inc.). Slides were viewed under a Zeiss LSM510 confocal microscope using a C-apochromat 40×/1.2 NA water immersion objective. Positive ANAs were further tested for their capacity to bind dsDNA of the trypanosoma *Crithidia luciliae* using an anti-nDNA antibody test kit (CrithiDNA; Antibodies Inc.) following the manufacturer's directions. The procedure is the same as that described for the ANA test.

DNA Microextraction and PCR Assays. Genomic DNA was purified from individual hybrids as previously described (26). Primers and conditions used for H and κ chain PCR assays have already been detailed (references 22, 23, 26, and Fig. 1). A LD/JHCH PCR was designed (see below) and used as a first approach to distinguish between 3H9V_H replacement (22) and somatic mutation because somatic mutation in the CDR3 of the 3H9 sd-tg was shown to prevent amplification in the LD/CDR3 PCR. All hybrids negative in the LD/CDR3 PCR were tested with the LD/JHCH PCR. This PCR is not as specific as the LD/CDR3 PCR, because the JHCH primer is not sd-tg specific, and the 3H9 leader primer binds V genes with similar leader sequences. Hence, 3H9 sd-tgs with mutations in CDR3 as well as V_H replacements where the invading V_H gene uses a 3H9-like leader sequence will be detected in this assay. All PCR amplifications were carried out in a TouchDown thermocycler (Hybaid).

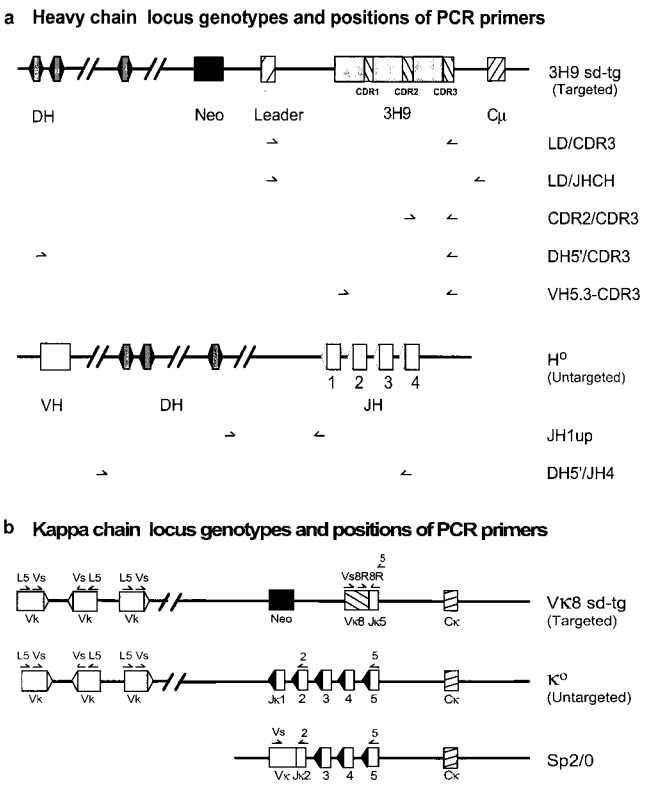

Figure 1. Positions of PCR primers in IgH and Igκ loci in 3H9Vκ8 mice. Locations of primers used to assess the rearrangement status of both targeted and untargeted H chain (a) and L chain (b) alleles are shown. H chain primers: LD, CDR2, and CDR3 are primers specific for the targeted H chain (12, 22). JHCH binds in the JH-CH intron of both H chain alleles (see Materials and Methods). DH5′ is a degenerate primer that binds 5′ of DH gene segments (except DSP.2 and DFL16.2) and can be used to detect D gene invasion (22) on the targeted allele and partial DJ rearrangements on the untargeted allele. VH5.3 is another degenerate primer specific for the FW3 of ~65% of V_H genes; VH5.3 is used to detect V_H replacement (22). The JH1 up primer set is used to detect unrearranged untargeted alleles. Any DJ rearrangement on this allele results in deletion of the JH1up sequence. L chain primers: 8R primers are specific for the targeted L chain (12, 23). Both Vs (28) and L5 (48) are forward Vκ primers; the former detects 80% of Vκ genes, and the latter 50–60%. Vs and L5 in combination with Jκ2 or Jκ5 reverse primers are used to detect Vκ-Jκ rearrangements. Sp2/0 L chain locus: Sp2/0 has been used as the hybridoma fusion partner (25). It harbors a nonproductive Vκ-Jκ2 rearrangement that is bound by Vs but not L5. Figures are not drawn to scale.

All primers were made by the Princeton University Synthesizing/Sequencing Facility.

V_H and Vκ Genomic DNA Sequencing. Genomic DNAs from individual hybridomas were used as templates from which to amplify V_H and Vκ genes. PCR amplifications were set up in a 30 μl vol containing 1 U of AmpliTaq Gold™ (Perkin Elmer) 1× buffer II, 200 μM of each dNTP (Boehringer Mannheim), 50 pmol of each primer, and 1.5 mM $MgCl_2$ (Perkin Elmer). The 5′ primers used to amplify V_H regions were either LD3H9 (5′-ctgtcaggaactgcaggtaagg-3′) or VH5.3 (5′-(g/c)aggt(g/t)cagctgcag(g/c)agtctgg-3′) in combination with a primer located in the JH–CH intron (JHCH: 5′-cttctctcagccggctccctc-3′). For PCR detection of Vκ genes, the forward primers were either specific for Vκ8 (MW133: 5′-ggtacctgtgggacattgtg-3′) or degenerate Vs (5′-ggctgcag(c/g)ttcagtggcagtgg(a/g)tc(a/t)gg(a/g)ac-3′) (28) and the reverse primer was a primer specific for the Jκ–Cκ intron (MW176: 5′-tgccacgtcaactgataatgagccctctc-3′). Amplifications were carried out with a thermal reactor (subambient Touch-Down; Hybaid) as follows: V_H: 92°C for 9 min, followed by 38 cycles of denaturation for 45 s at 94°C, annealing for 50 s at 56°C, extension for 1 min and 40 s at 72°C, and a final extension of 7 min at 72°C. Vκ8: 92°C for 9 min, followed by 38 cycles of denaturation for 30 s at 94°C, annealing for 30 s at 56°C, extension for 30 s at 72°C, and a final extension of 7 min at 72°C. Vs: 38 cycles of denaturation for 30 s at 94°C, annealing for 40 s at 65°C, extension for 1 min and 40 s at 72°C, and a final extension of 7 min at 72°C. Each fragment was size selected on a 1.5% agarose gel (Ultra Pure Agarose; GIBCO BRL) and purified by QIAquick gel extraction (Qiagen Inc.). Nucleotide sequencing was performed using the ABI Prism™ Big Dye™ Terminator Cycle Sequencing Ready Reaction Kit with AmpliTaq® DNA polymerase, FS, according to the manufacturer's directions (Applied Biotechnology, Inc.). Reactions were run on the Applied Biosystems 377 PRISM automated DNA sequencer (PE Applied Biosystems).

Vκ23 mRNA Sequencing. Total RNA was isolated from hybridomas using the RNAeasy kit (Qiagen Inc.), and 10 μg RNA was converted into cDNA using avian reverse transcriptase (Promega Corp.) and an oligo-dT/random hexamer primer mixture. 1 μl of cDNA was then amplified by PCR using Vs (28) as a forward primer and Cκ-specific primer as a reverse primer (Cκ: 5′-tggatggtgggaagatg-3′). The PCR program was as follows: 35 cycles consisting of 20 s at 94°C, 40 s at 55°C, and 90 s at 72°C. A Taq enzyme activation step of 9 min at 92°C was performed before the first cycle, and a final extension step of 7 min at 72°C ended the program. PCR products were purified on a gel with the QIAquick gel extraction kit (Qiagen Inc.) and were sequenced with the ABI prism system. For each sequence identified as Vκ23, cDNA was also amplified using a Vκ23 primer specific for the framework (FW)1 (Vκ23: 5′-gatattgtgctaactcagtctccagccac-3′) and the same Cκ-specific primer. PCR products were sequenced as described above.

Sequencing of MRL/lpr Vκ23 Germline Genes. Genomic DNA was extracted from the tails of two MRL-*lpr/lpr* mice as described above. 1 μl of DNA was used in a PCR containing 50 pmol of a Vκ23 forward primer specific for the FW1 region (Vκ23F: 5′-gatattgtgctaactcagtctccagccac-3′), 50 pmol of Vκ23 reverse primer complementary to the FW3 region (Vκ23R: 5′-gaggccagctgttactctgttg-3′), 1.5 mM $MgCl_2$, 200 μM dNTPs, 3 μl 10× buffer II, and 1 U AmpliTaq Gold™ (Perkin Elmer). The PCR program was as follows: 92°C for 9 min, followed by 35 cycles of denaturation for 30 s at 94°C, annealing for 30 s at 60°C, and extension for 40 s at 72°C. A final extension step at 72°C was carried out for 7 min. PCR products were size selected on a 1.5% agarose gel (Ultra Pure Agarose; GIBCO BRL) and purified with the QIAquick gel extraction kit (Qiagen Inc.). Purified DNA fragments were cloned into the pGEM®-T easy vector (Promega Corp.). JM109 competent cells were transformed by electroporation, and transformants were directly tested for the nature of the insert by PCR, using two different sets of Vκ23-specific primers. One set was made up of the Vκ23 primers used in the initial amplification (see above) and another set was made up of Vκ23 primers (Vκ23′F: 5′-gtgactccaggagatagc-3′; Vκ23′R: 5′-gttgataccagtgtaggtt-3′) specific for the new Vκ23 gene (Vκ23GL2) similar to our Vκ23 sequences (see text). Plasmid DNA from positive colonies of each group was sequenced as described above using a plasmid-specific T7 primer. Two Vκ23 germline se-

quences were identified. One was identical to the DP12 mAb sequence (4) and was not amplified by the second set of primers. The other one differed from the DP12 sequence by two nucleotides located in the FW1 and CDR2 (see Fig. 5) and was amplified with the Vκ23′ primers.

Sequence Analysis. Sequences were analyzed for homology to the original 3H9 and Vκ8 transgenes as well as to published Ig gene segments using EMBL/GenBank databases and Kabat et al. (29). The sequences of 3H9 V_H gene and the Vκ8 gene can be found in EMBL/GenBank/DDBJ databases under the accession numbers M18234 (3H9) and M34742 (Vκ8). The Vκ23 sequences described in this paper are available from EMBL/GenBank/DDBJ under the following accession numbers: AF139842–AF139849. The accession numbers for the V_H sequences presented in Fig. 3 B are AF145959–AF145963.

Statistical Analysis of Clonal Trees. We tested the hypothesis that mutations accumulated at the same rate and for equal duration at three loci. Under the assumption that all three loci mutate at the same rate, we reasoned that if the three genes had mutated for equal lengths of time, they should have equal numbers of mutations per base. We used the genealogical trees to determine the number of independent mutations (the total sum of the branch lengths in each tree) that occurred at each of the three loci. By this measure, 3H9, Vκ8, and Vκ23 loci accumulated $M_{3H9} = 34$, $M_{V\kappa8} = 33$, and $M_{V\kappa23} = 18$ mutations (see Fig. 6), respectively, in sequences of length of $L_{3H9} = 363$ bases, $L_{V\kappa8} = 339$ bases, and $L_{V\kappa23} = 324$ bases (see Figs. 3 A, 4, and 5). We used only mutations in the coding sequences for this analysis.

Assuming the hypothesis is true and an underlying Poisson distribution of mutations, we determined the mean number of mutations per base (λ_0) from the maximum likelihood estimate, in this case, the average:

$$\hat{\lambda}_0 = \left(\frac{M_{3H9} + M_{v\kappa8} + M_{v\kappa23}}{L_{3H9} + L_{v\kappa8} + L_{v\kappa23}}\right) = \frac{85}{1026} = 0.08285. \quad (1)$$

Under the null hypothesis (H_0: mutation for equal duration at three loci), the number of mutations in each sequence (M_{3H9}, etc.) would be determined by the same value of λ_0 mutations per base estimated by $\hat{\lambda}_0$ above. Our hypothesis amounts to equating the three individual mutation frequencies λ_{3H9}, $\lambda_{V\kappa8}$, and $\lambda_{V\kappa23}$ to a common frequency λ_0. Thus, the total number of mutations in the three sequence sets would be governed by Poisson distributions with means $\bar{M}_{3H9} = L_{3H9}\lambda_0$, $\bar{M}_{v\kappa8} = L_{v\kappa8}\lambda_0$, and $\bar{M}_{v\kappa23} = L_{v\kappa23}\lambda_0$. Put formally: H_0: $\lambda_{3H9} = \lambda_{v\kappa8} = \lambda_{v\kappa23} = \lambda_0$, i.e., all have the same number of mutations per base, meaning the same duration of mutation. We tested the alternative: H_A: $\lambda_{v\kappa23} < \lambda_{3H9} = \lambda_{v\kappa8}$ using the following statistic:

$$Z_0 = \frac{\left(\frac{M_{3H9} + M_{v\kappa8}}{L_{3H9} + L_{v\kappa8}}\right) - \left(\frac{M_{v\kappa23}}{L_{v\kappa23}}\right)}{\sqrt{\frac{(\hat{\lambda}_{3H9} + \hat{\lambda}_{v\kappa8})}{(L_{3H9} + L_{v\kappa8})^2} + \frac{\hat{\lambda}_{v\kappa23}}{(L_{v\kappa23})^2}}}. \quad (2)$$

The next section describes how Z_0 was derived. The alternative hypothesis includes the statement that $\lambda_{3H9} = \lambda_{v\kappa8}$, so we estimated their common value by:

$$\left(\frac{M_{3H9} + M_{v\kappa8}}{L_{3H9} + L_{v\kappa8}}\right) = \hat{\lambda}_{3H9} = \hat{\lambda}_{v\kappa8}. \quad (3)$$

$\hat{\lambda}_{v\kappa23}$ is estimated by $M_{v\kappa23}/L_{v\kappa23}$. Under H_0, these two formulas estimate the same quantity. Thus under H_0, the expectation of their difference:

$$\left(\frac{M_{3H9} + M_{v\kappa8}}{L_{3H9} + L_{v\kappa8}}\right) - \left(\frac{M_{v\kappa23}}{L_{v\kappa23}}\right) \quad (4)$$

is zero. To obtain a standardized (mean = zero, variance = one) statistic, namely Z_0, under H_0, we divided the difference by the square root of its estimated variance, which we calculated as follows. The variance of a difference is the sum of the terms' separate variances, which is:

$$Var\left(\frac{M_{3H9} + M_{v\kappa8}}{L_{3H9} + L_{v\kappa8}}\right) + Var\left(\frac{M_{v\kappa23}}{L_{v\kappa23}}\right) = \left(\frac{Var(M_{3H9} + M_{v\kappa8})}{(L_{3H9} + L_{v\kappa8})^2} + \frac{Var(M_{v\kappa23})}{(L_{v\kappa23})^2}\right) = \left(\frac{Var(M_{3H9}) + Var(M_{v\kappa8})}{(L_{3H9} + L_{v\kappa8})^2} + \frac{Var(M_{v\kappa23})}{(L_{v\kappa23})^2}\right). \quad (5)$$

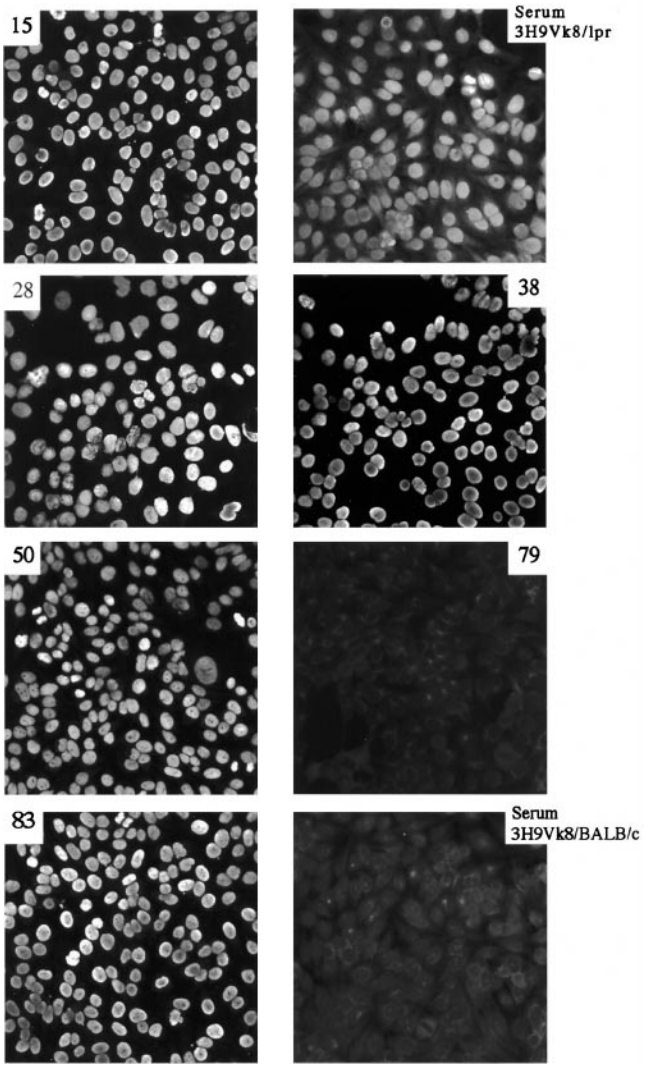

Figure 2. Immunofluorescence staining of HEp-2 cells by 3H9Vκ8/*lpr* serum and hybridoma supernatants. HEp-2 cells were incubated with supernatant from hybridomas (15, 28, 38, 50, 83, and 79) or 1:500 diluted serum from 3H9Vκ8/*lpr* and 3H9Vκ8/BALB/c mice. Serum Ig from 3H9Vκ8/*lpr* mice and all hybrids but 79 showed similar ANA patterns compatible with DNA or DNA–protein complex staining. Hybridoma 79 and sera from 3H9Vκ8/BALB/c mice gave the same negative pattern.

Table I. *Characterization of Hybridomas Derived from Anti-ssDNA sd-tg Mice in Both the MRL-lpr/lpr and the Nonautoimmune BALB/c Genetic Backgrounds*

Mouse	Genotype	Hybrids*			Isotype‡	DNA binding*‡	
		LD/CDR3	LD/JHCH	Sequencing	M/G	ssDNA§	dsDNA
3H9V κ8/*lpr*	$3H9^{+}V\kappa8^{+}$	33 (69)	38 (79)	38 (79)	26/7	25 (75)	4 (12)
	$3H9^{+}V\kappa8^{-}$	1 (2)	1 (2)	1 (2)	0/1	0 (0)	0 (0)
	$3H9^{-}V\kappa8^{+}$	12 (25)	7 (15)	7 (15)	3/9	0 (0)	5 (42)
	$3H9^{-}V\kappa8^{-}$	2 (4)	2 (4)	2 (4)	0/2	0 (0)	0 (0)
	Total	48 (100)	48 (100)	48 (100)	29/19	25 (52)	9 (19)
3H9V κ8/BALB/c	$3H9^{+}V\kappa8^{+}$	65 (88)	–	–	65/0	65 (100)	0
	$3H9^{+}V\kappa8^{-}$	1 (1)	–	–	1/0	0	0
	$3H9^{-}V\kappa8^{+}$	8 (11)	–	–	8/0	0	0
	$3H9^{-}V\kappa8^{-}$	0 (0)	–	–	0/0	0	0
	Total	74 (100)	–	–	74/0	65 (88)	0

Results are from a single mouse for each genetic background. Both mice express the H and L chain sd-tgs 3H9 and Vκ8 in a heterozygous state (3H9/+;Vκ8/+). The *lpr*-derived hybridomas were generated from unmanipulated splenic B cells, whereas the BALB/c hybrids were derived from in vitro LPS-stimulated splenocytes. DNA binding activities of hybridoma supernatants were determined by solution phase ELISA as described in Materials and Methods. Clonally related hybrids are included in this table.

*Numbers in parentheses refer to the percentage of hybrids in each category. Other numbers represent the number of hybrids testing positive or negative for 3H9 and Vκ8 sd-tgs by PCR as described in Materials and Methods. In the "sequencing" column, the actual number of hybrids in each category based on nucleotide sequences is given.

‡To ease comparison with the 3H9Vκ8 BALB/c data, the different categories of "DNA binding" and "Isotype" were presented in accordance with the LD/CDR3 PCR.

§ssDNA refers to the hybrids that secrete anti-ssDNA mAbs with no dsDNA activity.

Table II. *Genetic Characteristics of the IgG-secreting Hybridomas from a 3H9Vκ8/lpr Mouse*

Hybridoma	Subtype	dsDNA binding		H Chain			L Chain		
		dsDNA	ANA	VH gene	JH	Mut./Rep.	Vκ gene	Jκ	Mut./Ger.
50	IgG2a	+	+++	3H9	4	Mut	8; 23	5/2′	Mut
79	IgG2a	+++	–	3H9	4	Mut	8; 23	5/2′	Mut
15	IgG2a	+++	+++	3H9	4	Mut	8; 23	5/2′	Mut
83	IgG2a	+++	+++	3H9	4	Mut	8; 23	5/2′	Mut
28	IgG2a	+++	+++	3H9	4	Mut	8; 23	5/2′	Mut
38	IgG2a	+	+++	3H9	4	Mut	8; 23	5/2′	Mut
46	IgG1	++	–	3H9	4	Mut	8	5	Ger
16	IgG3	+	–	3H9	4	Mut	8	5	Mut
57	IgG1	+++	–	J558	4	Rep	8	5	Ger
85	IgG1	–	–	J558	4	Rep	8	5	Ger
13	IgG3	–	–	J558	4	Rep	8	5	Ger
1	IgG2b	–	–	7183	4	Rep	8	5	Mut
2	IgG1	–	–	7183	4	Rep	8	5	Mut
49	IgG1	–	–	ND	4	ND	8	5	Mut

Jκ2′ is an allelic variant of the Jκ2 segment that is found in MRL-*lpr/lpr* mice. The number of + symbols is a measure of the optical density (dsDNA) or intensity of fluorescence (ANA) obtained using the anti-dsDNA mAb (Mx3828) as a reference. Mx3828 was derived from a 3H9Vκ8/*lpr* mouse. Mut., mutated; Rep., replacement; Ger., unmutated in comparison to the Vκ8 sd-tg.

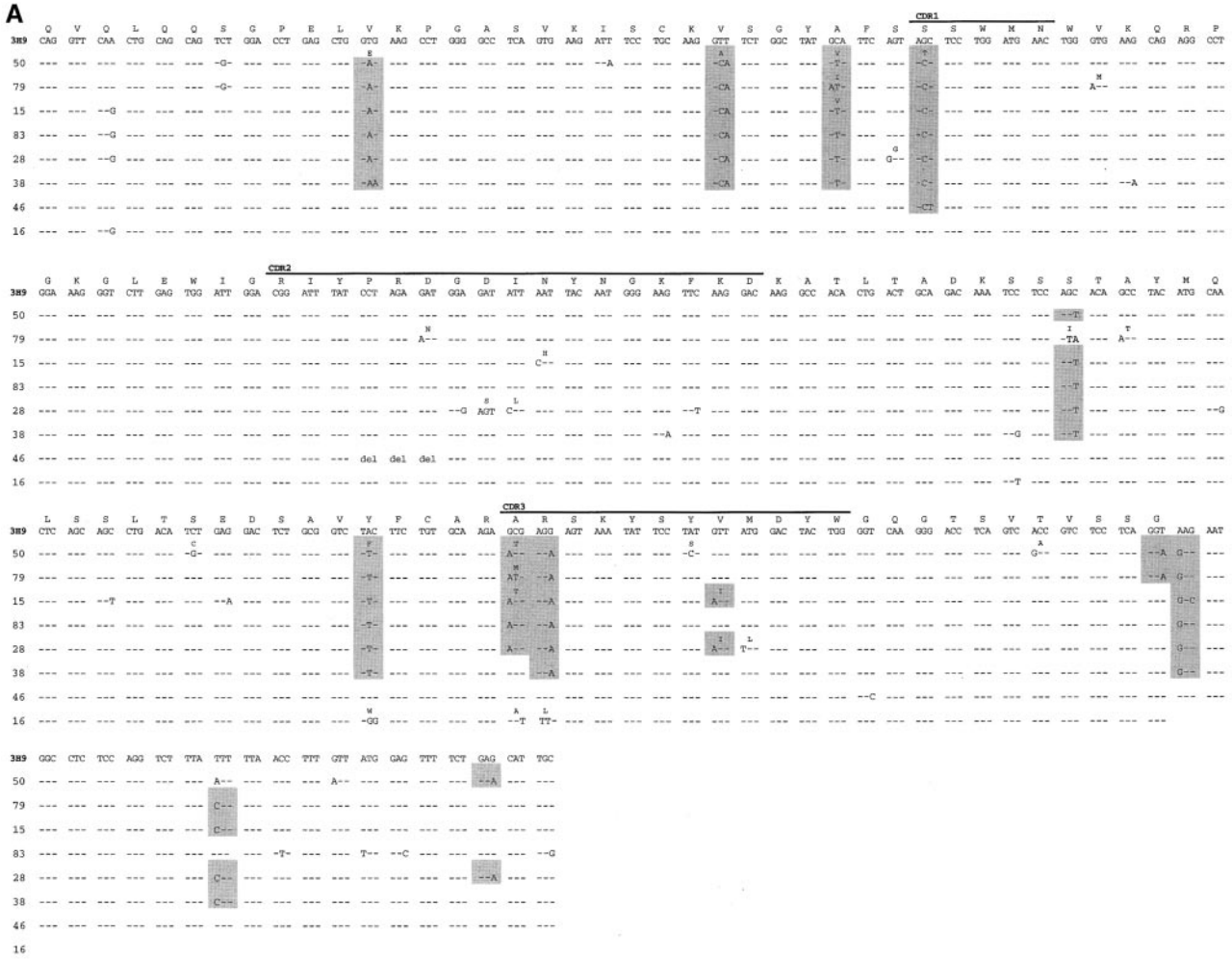

Figure 3 (continues on facing page).

The variance of a Poisson deviate is equal to its mean, thus,

$$Var(M_{3H9}) = \overline{M}_{3H9} = L_{3H9}\lambda_0 \qquad (6)$$

and similar formulas hold for $Var(M_{v\kappa 8})$ and $Var(M_{v\kappa 23})$. Thus, the variance of the difference is:

$$\frac{\lambda_{3H9} + \lambda_{v\kappa 8}}{(L_{3H9} + L_{v\kappa 8})^2} + \frac{\lambda_{v\kappa 23}}{(L_{v\kappa 23})^2}. \qquad (7)$$

This quantity is estimated by substituting the above estimates of the λ's for their true values. For these data, $Z_0 = 2.063$.

We sampled the Poisson distribution with parameters $\overline{M}_i$, i = 3H9, Vκ8, Vκ23 to obtain deviated M_{3H9}, $M_{v\kappa 8}$, and $M_{v\kappa 23}$, rigorously under H_0. From these, a new $\hat{\lambda}_0$ was obtained as above, and finally, a new value of Z was derived. If the new Z was at least Z_0, the event was tallied. The procedure was repeated 100,000 times. In these trials, Z_0 was equalled or exceeded only 1,780 times, requiring H_0 to be rejected at the 1.78% level.

Results

Anti-DNA Abs Arise Spontaneously in 3H9Vκ8/lpr Mice. In nonautoimmune mice, 3H9Vκ8 B cells are anergized. Consequently, 3H9Vκ8 transgenic mice have no detectable DNA binding activity in their serum (12). To assess whether such anergic B cells escape tolerance in autoimmune MRL/*lpr* mice, sera from 3H9Vκ8/*lpr* mice were tested for the presence of anti-DNA Abs. Anti-DNA Abs were readily detected by ELISA as well as by indirect immunofluorescence on *Crithidia luciliae* (data not shown). Furthermore, ANAs were detected in the sera of 3H9Vκ8/*lpr* as early as 2 mo of age. None of these Ab specificities was detected in sera from 3H9Vκ8/BALB/c mice (Fig. 2 and data not shown).

Anti-DNA B Cells Are Activated in 3H9Vκ8/lpr Mice. Hybridomas from 3H9Vκ8/*lpr* mice have many features that indicate 3H9Vκ8/*lpr* B cells are activated rather than anergic, as they are in the BALB/c background. Unmanipulated 3H9Vκ8/*lpr* B cells yield high frequencies of hybridomas, unlike 3H9Vκ8/BALB/c B cells, which require LPS stimulation or immunization for hybridoma formation. In this regard, 3H9Vκ8/*lpr* B cells are similar to those of diseased, nontransgenic, MRL/*lpr* mice that generally have high spontaneous fusion efficiencies (30). A high percentage of spontaneous hybridomas from diseased mice

Figure 3. Nucleotide and deduced amino-acid sequences of hybridoma H chains. (A) Sequences of the 3H9 sd-tg in IgG-secreting hybridomas (50, 79, 15, 83, 28, 38, 46, and 16). The sequence of the 3H9 sd-tg is shown. Identities are indicated with dashes. CDRs are defined according to Kabat et al. (29). Unmutated sequences from IgG-secreting hybridomas are not presented in this figure. Mutations shared by at least two sequences are shaded except for the first two, which result from the degenerate nature of the VH5.3 primer used in amplification. (B) V_H replacement sequences. In these hybridomas (57, 85, 13, 1, and 2), the 3H9 sd-tg has been replaced by an upstream V_H gene, via the embedded heptamer at the end of CDR3 in 3H9 (22). The sequence of the 3H9 sd-tg is used as a reference for the hybridomas 57, 85, and 13 because the replacing genes belong to the same J558 gene family. Boxed residues at positions 53, 57, and 65 are specific to the 3H9 gene (mutations). Identical nucleotides between hybridomas 57 and 85 are shaded when different from 3H9. These two hybrids represent potential members of the same clone (see text). The sequence of hybridoma 13 is also compared with the unmutated H chain sequence of mAb 19.1.2, which uses a more related J558 gene (sequence data available from EMBL/GenBank/DDBJ under accession number AJ223534). Identical nucleotides between hybridoma 13 and the reference J558 gene are also shaded. The D segment used in hybridoma 13 has homology with DQ52 (5′ boundary) and DSP2.6-c (3′ boundary) gene segments, probably resulting from a D–D fusion. Sequences from hybridomas 1 and 2 are compared with two different genes from the 7183 gene family, EMBL/GenBank/DDBJ accession numbers AF003722 and Z22078, respectively. In hybridoma 1, the D segment has homology with both the DSP2.9 (5′ boundary) and the DSP2.10-c (3′ boundary) gene segments, and in hybridoma 2, with both the DSP2.10 (5′ boundary) and the DFL16.1E (3′ boundary) gene segments. The regions of homology are underlined and identical nucleotides are in bold.

produce autoantibodies such as anti-DNA and RF suggesting that self-antigens are driving fusable B cells (31). Hybridoma panels from 3H9Vκ8/*lpr* mice also have high frequencies of anti-DNA-secreting B cells. For example, in one hybridoma panel derived from a 2-mo-old 3H9Vκ8/*lpr* mouse, 34 (71%) out of 48 hybridomas secreted anti-DNA Abs (Table I). This is not surprising given that the tg Ab binds ssDNA, but of these 34 hybridomas, 9 bound dsDNA in ELISA, and of these, 5 displayed a homogeneous nuclear staining pattern on HEp-2 cells (Fig. 2). Anti-dsDNA and ANAs are rarely found in hybridoma panels from LPS-activated B cells from 3H9Vκ8/BALB/c mice; instead, most of these hybridomas produce anti-ssDNA Abs (reference 13 and Table I). Finally, the presence of isotype-switched anti-DNA Abs in the serum of 3H9Vκ8/*lpr* and the secretion of IgG by 40% of the hybridomas (Tables I and II) are other indications of antigen activation. Strikingly, all the dsDNA/nuclear binders are IgG. Together, these results provide strong evidence that these mice are undergoing a (self-)antigen-driven immune response.

The Genetic Basis of Anti-DNA in 3H9Vκ8/lpr Mice: Mutation. Anti-dsDNA/ANAs in 3H9Vκ8/*lpr* mice could be generated either by somatic mutation or by gene replacement. To distinguish mutation from replacement, we examined the status of the H and L chain sd-tgs. Those hybridomas that retain both the 3H9 H and Vκ8 genes but express unique specificities are likely to be mutated. Those that have lost 3H9 and/or Vκ8 gene(s) would most likely

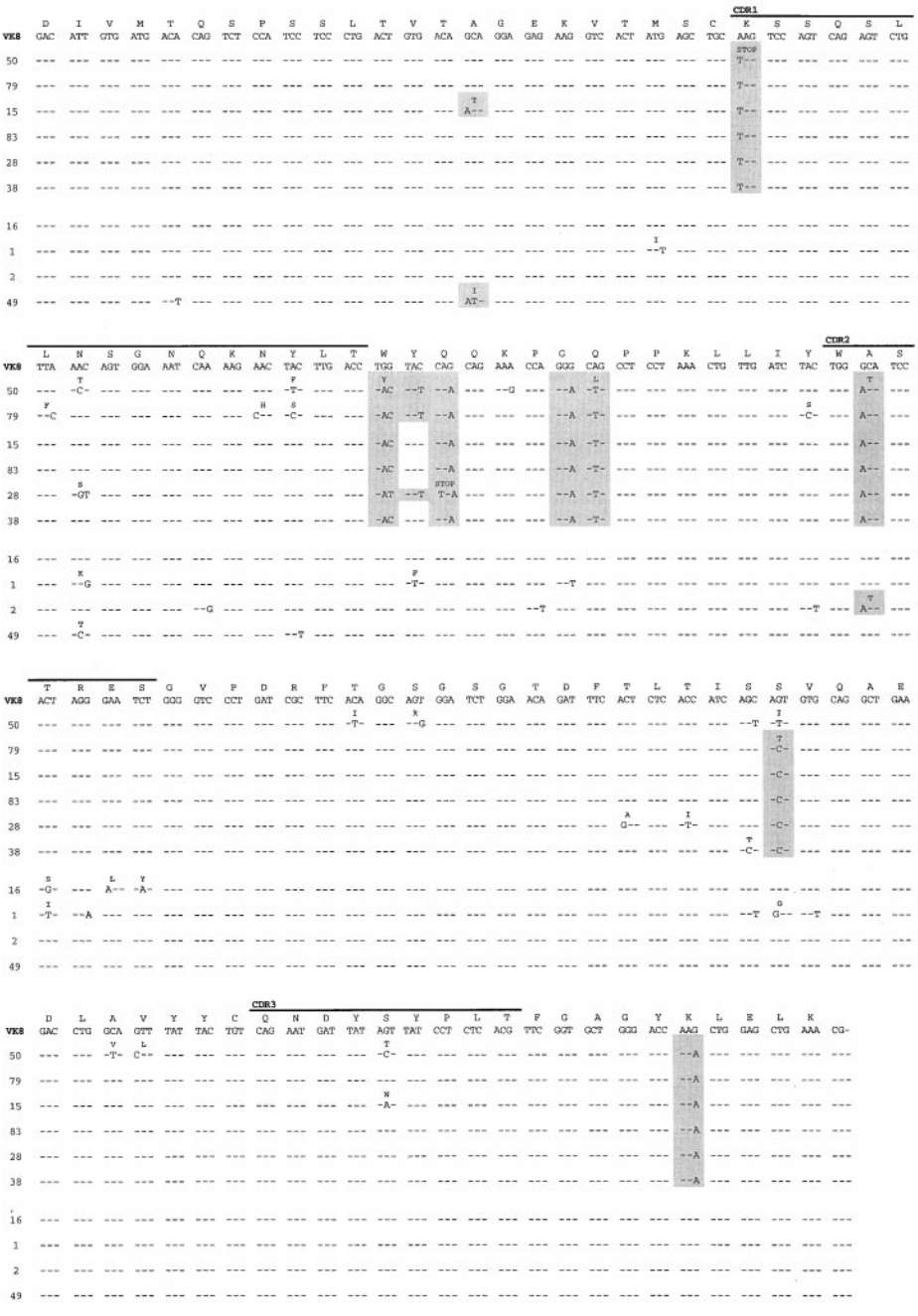

Figure 4. Nucleotide and deduced amino-acid sequences of the Vκ8 sd-tg in IgG-secreting hybridomas. The Vκ8 sd-tg sequence is used as a reference. Identities are indicated with dashes. CDRs are defined according to Kabat et al. (29). Mutations shared by at least two sequences are shaded. Only mutated Vκ8 sequences are presented (10 out of 46). Six sequences display a stop codon at the beginning of the CDR1.

have specificities generated de novo. We tested for the presence of V_H and Vκ transgenes in hybridomas from the 3H9Vκ8/*lpr* mouse using a series of PCR assays (Fig. 1). Out of 48 hybridomas studied, 38 (79%) were positive for both the 3H9 and Vκ8 genes. Of these double-positive hybridomas, some did not bind DNA, whereas others have acquired specificity for anti-dsDNA (Table I), suggesting that the 3H9 and/or Vκ8 transgenes have undergone somatic mutation. Similar results were obtained from a hybridoma panel of a 4-mo-old 3H9Vκ8/*lpr* mouse (Brard, F., and M. Weigert, unpublished data).

The V_H genes of 13 IgG-secreting hybridomas with changed specificity (anti-dsDNA/ANA$^+$ or non-anti-DNA) were amplified and sequenced. Of these, eight were 3H9$^+$Vκ8$^+$ mutants and five were 3H9$^-$Vκ8$^+$. Their nucleotide and deduced amino-acid sequences are shown in Fig. 3, A and B, and are summarized in Table II. Mutations in the 3H9 sd-tg are located both in the coding and in the noncoding regions. The average number of mutations per V region is high, 12.5, with the most mutated V region having 22 mutations (hybridoma 28) and the least mutated having 6 (hybridoma 16) (Fig. 3 A). In the JHCH intron, the average number of mutations within the 60 bp immediately 3′ of J_H4 is 2.4, with the most mutated sequence having 5 mutations. Of note, hybridoma 46 has a deletion of three codons in CDR2. In the same region, hybridoma

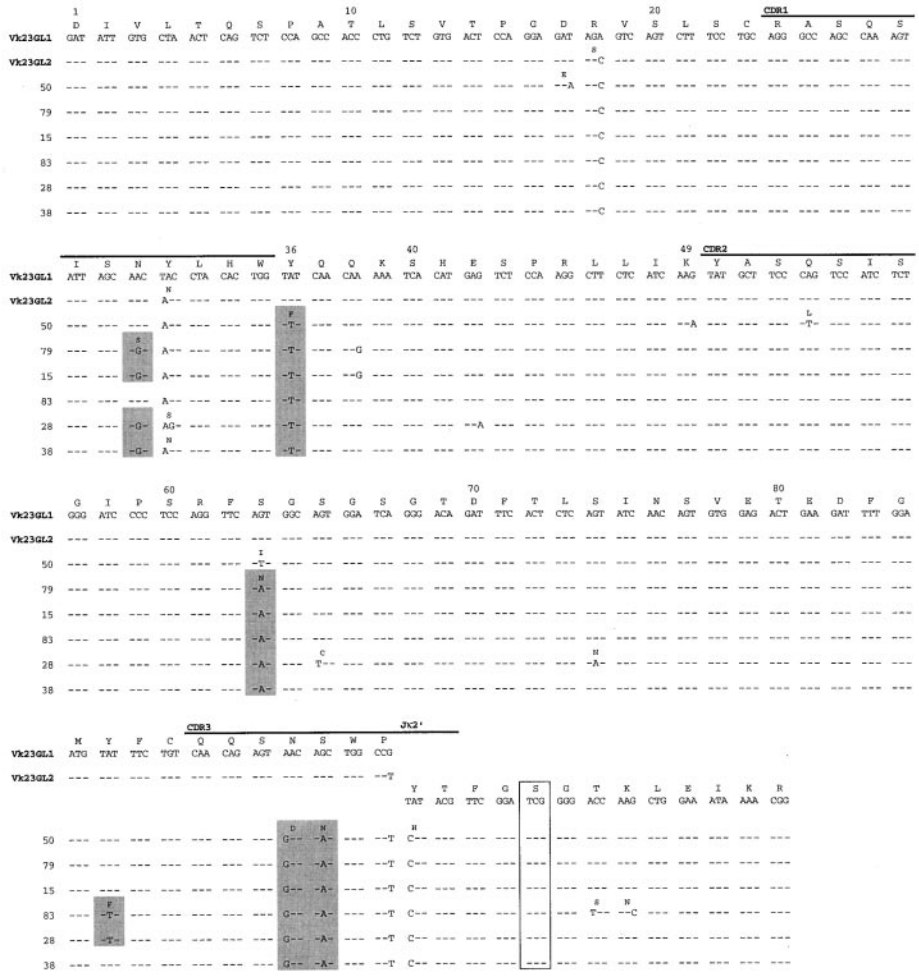

Figure 5. Nucleotide and deduced amino-acid sequences of Vκ23 from B cell clone members. Hybridomas that had a nonsense mutation in their Vκ8 gene were tested for the presence of another L chain by sequencing L chain mRNA. All six hybridomas express a Vκ23 L chain. These sequences are compared with two Vκ23 germline genes, Vκ23GL1 and Vκ23GL2, obtained from MRL/*lpr* tail DNA. Identities are indicated with dashes. Mutations shared by at least two members are shaded. T and C nucleotides located at the V-J junction are likely to result from the germline segments and therefore are not considered as mutations or N-additions. The CDRs are defined according to Kabat et al. (29). In all sequences, the Vκ23 gene is rearranged to a Jκ2′ gene segment. Jκ2′ is an MRL/*lpr* allelic variant of Jκ2 that occupies the same chromosomal position as Jκ2 relative to other Jκs. It has a serine at position 100 (boxed) instead of the glycine of Jκ2. The usage of a Jκ2′ segment demonstrates that the Vκ gene rearranged on the untargeted allele of the MRL/*lpr* mouse.

28 has a stretch of five nucleotides that are different from their germline counterparts. We think this most likely results from some form of insertion and deletion. Wilson et al. (32) described similar insertion/deletion mutants in Ig hypervariable loops. In their study, deletions occurred at tandem repeat sequences and inevitably destroyed one of the tandem repeats. Insertions usually involved duplications of the immediately adjacent sequence. In 3H9's CDR2, we have identified such a repeat sequence, AGA GAT GGA GAT, at the site of the insertion/deletion mutations. The deletion in hybridoma 46 removes one full repeat element plus one adjacent codon. The sequence of the insertion in hybridoma 28, GAGTC, is similar to the repeat motif GAGAT. Interestingly, the GAGAT motif contains the putative hot spot sequence RGYW (33), and it is known that deletion/insertion events usually occur in the vicinity of mutational hot spots (32).

Mutations were also found in 10 of the Vκ8 sd-tgs (Fig. 4). Here again, mutations were found throughout the sequence. The average number of mutations per V region was 9.2, ranging from 18 mutations (hybridoma 50) to 3 mutations (hybridoma 16). All together, many of the V_H and V_L genes sequenced from the hybridomas presented in Table II have replacement mutations in CDRs. Thus, it is possible that the novel specificities of these antibodies are the result of mutation in the 3H9 and/or Vκ8 genes.

Clonal Expansion. Hybridomas 50, 79, 15, 83, 28, and 38 share eight mutations in their 3H9 sequences, therefore it is likely that they come from an expanded B cell clone. Ordinarily, B cells are defined as members of a clone based not only on the presence of shared mutations but also on sequence identity of V_HCDR3. However, sequence identity of V_HCDR3 is not an applicable criterion by which to judge clonality in transgenic models. Nevertheless, the following observations indicate that these six hybridomas are indeed derived from a single B cell clone: first, these hybridomas all express the same isotype, IgG2a. Second, these hybridomas also share 15 mutations in their Vκ8 and 3H9 sd-tgs, collectively. Third, each of these hybridomas maintains a germline H chain allele and has identical endogenous κ chain rearrangements (see below). Furthermore, it is unlikely that the shared mutations are entirely the result of positive selection and/or hotspot mutation, because only two of these shared mutations are found in the sequences of hybridomas that we know to be unrelated on the basis of rearrangement status (hybridoma 46, Fig. 3 A, and hybri-

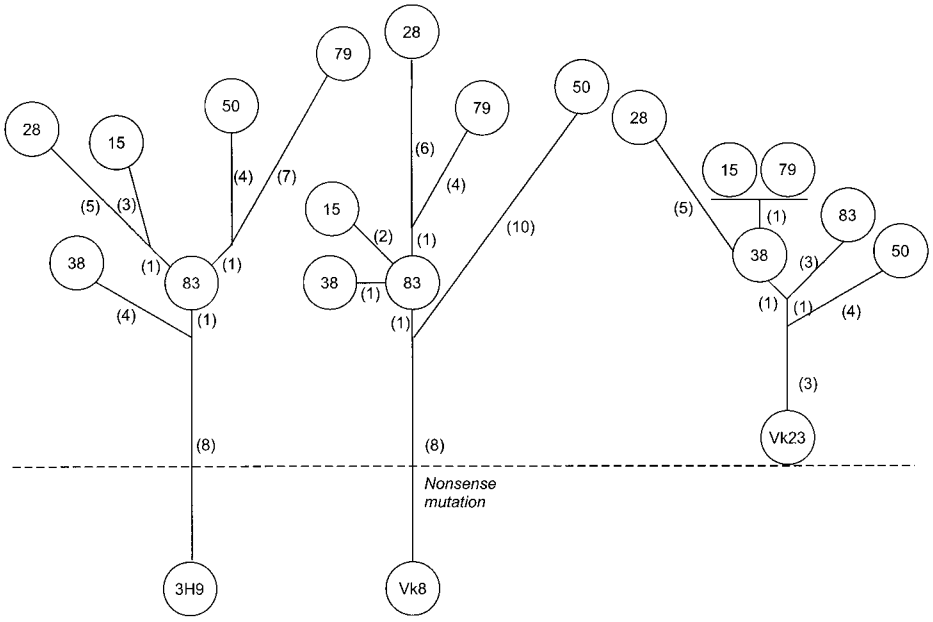

Figure 6. Genealogical relationships between antinuclear B cells from a 3H9Vκ8/*lpr* mouse. Genealogical trees based on the coding sequences of the 3H9 (A), Vκ8 (B), and Vκ23 (C) genes from the clonally related hybridomas are shown. The trees are constructed from patterns of shared and unique mutations by assuming that shared mutations represent single events and not independent parallel mutations and by assuming the minimum number of mutational events. To construct the 3H9 and Vk8 trees, it was sometimes necessary to assume that a specific nucleotide underwent two different mutations. For example, in the 3H9 tree we assumed all members of the clone originally had the silent C→T mutation in the serine of FW3 and that subsequently hybridoma 79 underwent a T→A mutation at the same position. This explains why there are eight shared mutations in the stem of the 3H9 tree, whereas Fig. 3 A shows only seven coding region mutations shared by all members of the clone. The length of the line between each B cell is proportional to the number of mutations (given in parentheses). Note the similar shapes and branch morphology of the three trees.

doma 2, Fig. 4); moreover, 7 out of the 15 shared mutations in both H and L transgenes are nonselectable, either because they are silent or because they occur in introns.

The most interesting feature of this clone is that all members share a mutation to the TAG nonsense codon in the Vκ8 sd-tg at the beginning of the CDR1 (Fig. 4). Because these clones secrete an IgG2a/κ Ab, the untargeted κ allele must be rearranged and expressed. To determine the nature of the expressed L chain, Vκ mRNA from these six hybridomas was sequenced (Fig. 5, Table II). All express a Vκ23 gene joined to Jκ2′, the MRL counterpart of Jκ2. Analysis of the V–J junction revealed that the first codon of Jκ2′ is deleted and a histidine is found in its place. This unusual junction has previously been observed in other Vκ23Jκ2′ sequences (18, 34). The histidine found at the junction may derive from either the end of the germline Vκ23 gene or the nucleotides immediately 3′ of the Vκ23 gene.

To evaluate the number of mutations in the Vκ23 sequences, it was necessary to determine the germline sequence of the Vκ23 gene. Because GenBank did not contain an appropriate sequence, we cloned Vκ23 genes from MRL/*lpr* tail DNA. Two potential candidates, Vκ23GL1 and Vκ23GL2 (Fig. 5) were identified. Our six hybridoma Vκ23 sequences are most similar to Vκ23GL2. Assuming that Vκ23GL2 is the bona fide germline counterpart, the Vκ23 sequences from our hybridomas had an average of 6.5 mutations per V region, with the most mutated V region having 10 mutations (hybridoma 28) and the least mutated having 5 (hybridomas 38 and 83). These six sequences have three mutations in common, and two other mutations are shared by at least four out of the six clone members.

The shared V_H and V_κ mutations form a hierarchy characteristic of expanded clones. This hierarchy of mutations allowed us to construct a genealogy of the clone members (Fig. 6). The 3H9 and Vκ8 trees have roughly the same height and shape. This similarity illustrates that the onset and rate of mutation are the same in H and L chain genes. Although the Vκ23 tree has a "branch morphology" similar to that of the 3H9 and Vκ8 trees, it appears to have a shorter "trunk." Furthermore, the average number of mutations is less in Vκ23 than in either 3H9 or Vκ8 (6.5 compared with 14 and 13, respectively). These results indicate that the Vκ23 L chain started to mutate later than the Vκ8 or 3H9 transgenes, but that once initiated, Vκ23 mutation proceeded at a similar rate. Taken together, these mutation patterns and tree shapes imply that the Vκ23 gene was rearranged and expressed after the onset of mutation in the 3H9 and Vκ8 transgenes.

To confirm this conclusion, a statistical analysis testing the hypothesis that mutations accumulated for equal durations at the three loci was performed. Implicit in this calculation is the assumption, based on the absence of clear evidence to the contrary, that the mutation rate was equal at each of these three loci. We also assumed that the number of mutations found in each tree would be Poisson distributed. We estimated mutation frequencies per base from the number of mutations divided by the number of bases in the corresponding sequence set. The frequency estimates for our 3H9 and Vκ8 trees did not differ significantly, and in fact were very close to each other. We combined the 3H9 and Vκ8 data and compared their combined frequency estimate to that obtained for the Vκ23 sequences. To test the significance of this difference, we combined all three data

sets for an overall estimate of mutation frequency. We then simulated mutations in the three trees by generating Poisson deviates with means adjusted for each gene's particular sequence length. We tallied the number of times the difference in mutation frequencies observed this way, (i.e., rigorously, under the null hypothesis of identical mutation durations for each sequence), was as large or larger than their actual observed difference. Their observed difference was equalled or exceeded in only 1.78% of 100,000 trials. This allowed us to reject the hypothesis that all three Ig loci mutated for equal duration ($p = 0.0178$). Therefore, we conclude that the Vκ23 L chain gene was rearranged in the periphery and then started to undergo somatic mutation.

All members of this clone have acquired dsDNA specificity, and five out of six are ANA^+ (Fig. 2). The acquisition of dsDNA and antinuclear activity could be due to mutation in either 3H9 or Vκ23. In particular, the mutations to asparagine in FW3 and CDR3 in Vκ23 might create anti-DNA specificity (35). Alternatively, the Vκ23 L chain itself may create the ANA specificity (Table II), since ANAs and antihistone antibodies derived from autoimmune mice are often associated with Vκ23 L chains (18, 19, 34, 36–38).

Discussion

Earlier studies examined the regulation of the 3H9 H chain tg in *lpr/lpr* mice (18, 19). The 3H9 H chain transgenic without an accompanying L chain transgene is an excellent model for studying tolerance and loss thereof: the V_H gene coding for 3H9 is the most popular V_H among disease-associated anti-DNAs, constituting ~20% of the >200 sequenced anti-DNAs from MRL/*lpr*, (NZB × NZW)F_1 and (NZB × SWR)F_1. An unusual but useful feature of 3H9 (and other anti-DNA H chains) is that association with different L chains modifies DNA binding. 3H9/L chain combinations fall into three broad classes: combinations that sustain ss/dsDNA like that of the original 3H9/Vκ4 combination, combinations that modify DNA binding as in the 3H9/Vκ8 combination that only binds ssDNA, and combinations that veto DNA binding as, for example, 3H9/Vκ12/13. A study of 3H9 H chain in combination with a broad variety of endogenous L chains shows that the proportion of the three classes is ~30% ds/ss : 60% ss : 10% non-DNA binding (39). Moreover, certain L chains in combination with 3H9 yield unique ANA patterns as illustrated in Fig. 2 for the 3H9/Vκ23 combination (21). Thus, 3H9 sd-tg mice yield a spectrum of antibodies, making the 3H9 sd-tg MRL/*lpr* a multipurpose system for studying the breakdown of tolerance. As might have been predicted, 3H9 tg *lpr/lpr* mice express the types of anti-DNAs that are ordinarily edited or inactivated. These include anti-ds/ssDNA and antibodies that are ANA^+. But a limitation of this model is that the precursor to the pathogenic anti-DNAs expressed in this *lpr/lpr* tg cannot be established; hence, the site(s) at which tolerance is broken is unknown. The advantage of the 3H9Vκ8/*lpr* mice described here is that the anti-DNA repertoire is limited to one specificity, anti-ssDNA, that in normal mice is known to be regulated by anergy (12, 14). That anti-dsDNAs are now expressed in the 3H9Vκ8/*lpr* means either that anergic cells become activated or that anergy cannot be established in *lpr/lpr* mice. Based on the evidence for Fas-mediated regulation of peripheral B cells (40, 41), we favor the latter interpretation.

The failure to establish or maintain anergy of anti-ssDNA leaves the *lpr/lpr* mouse with a population of B cells poised for the transition to autoimmune disease. Both in vivo and in vitro studies have shown that anti-DNAs such as 3H9Vκ8 can be substrates for mutation to dsDNA and nuclear antigen binding antibodies (39, 42). Here we show that this transition takes place during clonal expansion of 3H9Vκ8 B cells and results in the production of anti-dsDNA and ANAs typical of disease. In this regard, our results recapitulate the nature of MRL/*lpr* and other autoimmune mice. But, during clonal expansion 3H9Vκ8/*lpr* B cells are actually subjected to two forms of somatic diversification: first, expanded hybridomas have accumulated a high frequency of mutations. These include mutations to R and N that could account for the shift of 3H9Vκ8 specificity from ssDNA to ss/dsDNA and the acquisition of antinuclear specificity (ANA^+, Fig. 2). The second form of diversification is L chain editing. This event is an indirect consequence of mutation: all members of the clone share a nonsense mutation in the Vκ8-Jκ5 gene, therefore IgGκ secretion requires L chain expression from the untargeted allele. This novel mechanism rescues a defunct B cell. Alternative explanations for this genotype, such as coexpression of both κ genes throughout the lifetime of the clone, are highly unlikely ($p \leq 0.0178$, see Materials and Methods).

V gene rearrangement during clonal expansion is not surprising in view of the evidence for RAG expression in germinal centers (43–45). But the relevance of RAG-mediated recombination to the immune response at this stage of B cell development has not been established. RAG-induced DNA nicks (45) may just be another manifestation of programmed cell death. It is unlikely that secondary rearrangement would enhance an ongoing immune response, because changing either H or L usually will produce a new specificity (29). Moreover, these new specificities will rarely, if ever, be propagated because of the lack of antigen and T cell help. Instead, RAG expression in germinal centers simply may be a gratuitous part of impending or actual cell death. This is suggested by the work of Hikida et al., who have shown that most of the B cells in germinal centers that express RAG are undergoing apoptosis (46). In fact, apoptosis may have been the raison d'être for RAG to begin with. The earliest B and/or T cell receptor genes were probably intact V genes, not segmented V, D, and J genes. These genes may have included sequences homologous to recombination signals, and primitive vertebrates may have fixed genes coding for proteins that cut DNA at these sites. Such cuts may have served to inactivate V genes or even to kill cells, thereby enforcing allelic exclusion and/or helping to maintain steady state levels of lymphocytes.

For a defunct B cell to be rescued by secondary rearrangement requires truly exceptional circumstances, but anti-DNAs such as 3H9/Vκ8 provide the conditions for rescue. First, L chain replacement does not always destroy DNA binding, because the H chain makes most of the antibody contacts to DNA (42). Hence, specificity for DNA can be maintained or modified even though Vκ8 is replaced (i.e., a kind of impotent receptor editing). Second, the self-specificity of 3H9/Vκ8 (and the L chain alternatives that, with 3H9H chain, sustain DNA binding) ensures that these antibodies will always be exposed to a cognate antigen. That germinal centers are sites of apoptosis is relevant to this point because the germinal centers are considered possible sites where the target lupus autoantigens may be presented. Third, DNA can be thought of as a superantigen, in the sense that it is associated with a wide variety of both self- and foreign proteins. Thereby, as long as a B cell's receptor binds DNA, that B cell can present a variety of T cell epitopes derived from these DNA-associated proteins. Take, for example, a receptor directed to the complex of DNA–histone. Even though L chain replacement converts the receptor to one that only binds DNA, the receptor will still bind chromatin and ultimately that B cell can present histone peptides. Thus, this kind of autoantibody will rarely be at a loss for T cell help. 3H9/Vκ8 descendents illustrate this strategy: the 3H9/Vκ23 receptor has acquired specificity for dsDNA yet still binds ssDNA, making it so that the revised B cell can still present the same T cell epitope(s) as the parental 3H9/Vκ8 B cell.

These studies show that expression of anti-DNA in Fas-deficient mice is influenced in at least two ways: first, B cells that are anergic in normal mice become activated; second, anti-DNA antibodies can arise in defunct B cells by V gene replacement. Both processes lead to the development of a spectrum of autoantibodies. Activation of anti-ssDNA B cells leads to clonal expansion and mutation and some of these mutations lead to specificity for dsDNA. Thus, anergy is a major tolerance checkpoint in that it prevents low affinity anti-DNAs from mutating to pathogenic types. Secondary V gene rearrangement in B cells generates a new spectrum of specificities that will surely include autospecificities. These might be formed by novel VH/VL combinations as in antibodies associated with Vκ23.

The fact that secondary rearrangements, or editing, create autoreactivity in the autoimmune MRL/lpr is paradoxical, because in normal B cell development each round of editing adds to the number of non-autoreactive, mature B cells an animal can generate from a given set of precursor cells. How can one account for this difference? The answer must lie in a cell's "motivation" for continuing to rearrange. An immature B cell from a normal individual wants to make a functional receptor that does not bind too strongly to surrounding (self-)antigens. A mature cell from an autoimmune individual, on the other hand, is attempting to secure positive selection signals by rearranging until it has a receptor that binds an antigen with high avidity. This notion stems from the work of Hertz et al., who have shown that mature B cells experiencing low affinity interactions with antigen tend to initiate recombination, whereas high affinity antigen interactions abolish recombinase activity in mature B cells (47). They also point out that this type of peripheral regulation of receptor editing would tend to promote autoreactivity. What is not thoroughly considered by their work is the role of T cell help. And this is what may be special in the case of autoreactivity, especially of autoreactivity to DNA. Rescue of a cell that has become autoreactive through editing rearrangement in the periphery also requires T cell help (specific for autoantigens) that is extant in autoimmune mice.

Genes that affect the death of autoreactive cells and the disposal of defunct B cells (such as the *fas* gene) have a broad influence on the regulation of autoimmunity. In addition to extending the survival (and subsequent activation) of anergic B cells, they may also permit the development of an inappropriate repertoire by secondary rearrangement. The ability to detect peripheral editing in MRL mice is probably greatly enhanced by the *lpr* mutation that extends the life of B cells which otherwise would die before having had enough time to make a new receptor. Moreover, genes involved in cell death may regulate the concentration or availability of self-antigen. Casciola Rosen et al. have shown that the self-antigens targeted in lupus are found on the surface of apoptotic cells (6). This led them to suggest that failure to kill cells efficiently could influence self-tolerance by limiting the amount of self-antigen. This limitation may be particularly strict in the bone marrow microenvironment where the preimmune repertoire is developed. A shortage of tolerogen could explain why the spectrum of autoantibodies in systemic autoimmunity is biased toward molecules released during cell death and could also resolve the differences between regulation of antibodies directed to facultative and constitutive self-antigens.

The authors thank Sandra Jainandunsing for her excellent technical assistance, Joseph Goodhouse for help with the microscopy, and Daniel Lee for help with Fig. 2. We are grateful to all members of the lab for helpful comments on the manuscript. We also acknowledge the CORE Services of Princeton University for oligonucleotide synthesis, DNA sequencing, and animal colony care.

F. Brard was supported in part by the Institut National de la Sante et de la Recherche Medicale and in part by the Fondation pour la Recherche Medicale and the Conseil regional de Haute-Normandie. M. Shannon is supported by the American Heart Association (9704047A) and M. Weigert is the recipient of National Institutes of Health grant (GM20964-24).

Address correspondence to Martin Weigert, Department of Molecular Biology, Princeton University, Princeton, New Jersey 08544. Phone: 609-258-2683; Fax: 609-258-2205; E-mail: mweigert@molbio.princeton.edu

Submitted: 29 March 1999 Revised: 23 June 1999 Accepted: 28 June 1999

References

1. Tan, E.M. 1988. Antinuclear antibodies: diagnostic markers and clues to the basis of systemic autoimmunity. *Pediatr. Infect. Dis. J.* 7(Suppl):S3–S9.
2. Hardin, J.A. 1986. The lupus autoantigens and the pathogenesis of systemic lupus erythematosus. *Arthritis Rheum.* 29: 457–460.
3. Shlomchik, M.J., A. Marshak-Rothstein, C.B. Wolfowicz, T.L. Rothstein, and M.G. Weigert. 1987. The role of clonal selection and somatic mutation in autoimmunity. *Nature.* 328:805–811.
4. Shlomchik, M., M. Mascelli, H. Shan, M.Z. Radic, D. Pisetsky, A. Marshak-Rothstein, and M. Weigert. 1990. Anti-DNA antibodies from autoimmune mice arise by clonal expansion and somatic mutation. *J. Exp. Med.* 171:265–292.
5. Craft, J.E., and J.A. Hardin. 1987. Linked sets of antinuclear antibodies: what do they mean? *J. Rheumatol.* 14(Suppl): 106–109.
6. Casciola Rosen, L.A., G. Anhalt, and A. Rosen. 1994. Autoantigens targeted in systemic lupus erythematosus are clustered in two populations of surface structures on apoptotic keratinocytes. *J. Exp. Med.* 179:1317–1330.
7. Nemazee, D., and K. Buerki. 1989. Clonal deletion of autoreactive B lymphocytes in bone marrow chimeras. *Proc. Natl. Acad. Sci. USA.* 86:8039–8043.
8. Hartley, S.B., J. Crosbie, R. Brink, A.B. Kantor, A. Basten, and C.C. Goodnow. 1991. Elimination from peripheral lymphoid tissues of self-reactive B lymphocytes recognizing membrane-bound antigens. *Nature.* 353:765–769.
9. Goodnow, C.C., J. Crosbie, S. Adelstein, T.B. Lavoie, S.J. Smith-Gill, R.A. Brink, H. Pritchard-Briscoe, J.S. Wotherspoon, R.H. Loblay, K. Raphael, et al. 1988. Altered immunoglobulin expression and functional silencing of self-reactive B lymphocytes in transgenic mice. *Nature.* 334:676–682.
10. Gay, D., T. Saunders, S. Camper, and M. Weigert. 1993. Receptor editing: an approach by autoreactive B cells to escape tolerance. *J. Exp. Med.* 177:999–1008.
11. Tiegs, S.L., D.M. Russell, and D. Nemazee. 1993. Receptor editing in self-reactive bone marrow B cells. *J. Exp. Med.* 177:1009–1020.
12. Erikson, J., M.Z. Radic, S.A. Camper, R.R. Hardy, C. Carmack, and M. Weigert. 1991. Expression of anti-DNA immunoglobulin transgenes in non-autoimmune mice. *Nature.* 349:331–334.
13. Chen, C., E. Luning Prak, and M. Weigert. 1997. Editing disease-associated autoantibodies. *Immunity.* 6:97–105.
14. Xu, H., H. Li, E. Suri Payer, R.R. Hardy, and M. Weigert. 1998. Regulation of anti-DNA B cells in recombination-activating gene–deficient mice. *J. Exp. Med.* 188:1247–1254.
15. Rathmell, J.C., and C.C. Goodnow. 1994. Effects of the lpr mutation on elimination and inactivation of self-reactive B cells. *J. Immunol.* 153:2831–2842.
16. Kench, J.A., D.M. Russell, and D. Nemazee. 1998. Efficient peripheral clonal elimination of B lymphocytes in MRL/*lpr* mice bearing autoantibody transgenes. *J. Exp. Med.* 188: 909–917.
17. Rubio, C.F., J. Kench, D.M. Russell, R. Yawger, and D. Nemazee. 1996. Analysis of central B cell tolerance in autoimmune-prone MRL/*lpr* mice bearing autoantibody transgenes. *J. Immunol.* 157:65–71.
18. Roark, J.H., C.L. Kuntz, K.A. Nguyen, A.J. Caton, and J. Erikson. 1995. Breakdown of B cell tolerance in a mouse model of systemic lupus erythematosus. *J. Exp. Med.* 181: 1157–1167.
19. Roark, J.H., C.L. Kuntz, K.A. Nguyen, L. Mandik, M. Cattermole, and J. Erikson. 1995. B cell selection and allelic exclusion of an anti-DNA Ig transgene in MRL-*lpr*/*lpr* mice. *J. Immunol.* 154:4444–4455.
20. Nagata, S., and P. Golstein. 1995. The Fas death factor. *Science.* 267:1449–1456.
21. Radic, M.Z., M.A. Mascelli, J. Erikson, H. Shan, and M. Weigert. 1991. Ig H and L chain contributions to autoimmune specificities. *J. Immunol.* 146:176–182.
22. Chen, C., Z. Nagy, E. Luning Prak, and M. Weigert. 1995. Immunoglobulin heavy chain gene replacement: a mechanism of receptor editing. *Immunity.* 3:747–755.
23. Luning Prak, E., and M. Weigert. 1995. Light chain replacement: a new model for antibody gene rearrangement. *J. Exp. Med.* 182:541–548.
24. Chan, O., and M.J. Shlomchik. 1998. A new role for B cells in systemic autoimmunity: B cells promote spontaneous T cell activation in MRL-*lpr*/*lpr* mice. *J. Immunol.* 160:51–59.
25. Kohler, G. 1980. Immunoglobulin chain loss in hybridoma lines. *Proc. Natl. Acad. Sci. USA.* 77:2197–2199.
26. Luning Prak, E., M. Trounstine, D. Huszar, and M. Weigert. 1994. Light chain editing in κ-deficient animals: a potential mechanism of B cell tolerance. *J. Exp. Med.* 180:1805–1815.
27. Radic, M.Z., J. Erikson, S. Litwin, and M. Weigert. 1993. B lymphocytes may escape tolerance by revising their antigen receptors. *J. Exp. Med.* 177:1165–1173.
28. Schlissel, M.S., and D. Baltimore. 1989. Activation of immunoglobulin kappa gene rearrangement correlates with induction of germline kappa gene transcription. *Cell.* 58:1001–1007.
29. Kabat, E.A., T.T. Wu, H.M. Perry, K.S. Gottesman, and C. Foeller. 1991. Sequences of Proteins of Immunological Interest. Fifth Edition. U.S. Department of Health and Human Services, Bethesda, MD. 2180 pp.
30. Wolfowicz, C.B., P. Sakorafas, T.L. Rothstein, and A. Marshak Rothstein. 1988. Oligoclonality of rheumatoid factors arising spontaneously in *lpr*/*lpr* mice. *Clin. Immunol. Immunopathol.* 46:382–395.
31. Shan, H., M.J. Shlomchik, A. Marshak Rothstein, D.S. Pisetsky, S. Litwin, and M.G. Weigert. 1994. The mechanism of autoantibody production in an autoimmune MRL/*lpr* mouse. *J. Immunol.* 153:5104–5120.
32. Wilson, P.C., O. de Bouteiller, Y.J. Liu, K. Potter, J. Banchereau, J.D. Capra, and V. Pascual. 1998. Somatic hypermutation introduces insertions and deletions into immu-

noglobulin V genes. *J. Exp. Med.* 187:59–70.
33. Rogozin, I.B., and N.A. Kolchanov. 1992. Somatic hypermutagenesis in immunoglobulin genes. II. Influence of neighbouring base sequences on mutagenesis. *Biochim. Biophys. Acta.* 1171:11–18.
34. Bloom, D.D., J.L. Davignon, M.W. Retter, M.J. Shlomchik, D.S. Pisetsky, P.L. Cohen, R.A. Eisenberg, and S.H. Clarke. 1993. V region gene analysis of anti-Sm hybridomas from MRL/Mp-*lpr*/*lpr* mice. *J. Immunol.* 150:1591–1610.
35. Radic, M.Z., and M. Weigert. 1994. Genetic and structural evidence for antigen selection of anti-DNA antibodies. *Annu. Rev. Immunol.* 12:487–520.
36. Monestier, M. 1991. Variable region genes of anti-histone autoantibodies from a MRL/Mp-*lpr*/*lpr* mouse. *Eur. J. Immunol.* 21:1725–1731.
37. Westhoff, C.M., A. Whittier, S. Kathol, J. McHugh, C. Zajicek, L.D. Shultz, and D.E. Wylie. 1997. DNA-binding antibodies from viable motheaten mutant mice: implications for B cell tolerance. *J. Immunol.* 159:3024–3033.
38. Tillman, D.M., N.T. Jou, R.J. Hill, and T.N. Marion. 1992. Both IgM and IgG anti-DNA antibodies are the products of clonally selective B cell stimulation in (NZB × NZW)F_1 mice. *J. Exp. Med.* 176:761–779.
39. Ibrahim, S.M., M. Weigert, C. Basu, J. Erikson, and M.Z. Radic. 1995. Light chain contribution to specificity in anti-DNA antibodies. *J. Immunol.* 155:3223–3233.
40. Rothstein, T.L., J.K. Wang, D.J. Panka, L.C. Foote, Z. Wang, B. Stanger, H. Cui, S.T. Ju, and A. Marshak Rothstein. 1995. Protection against Fas-dependent Th1-mediated apoptosis by antigen receptor engagement in B cells. *Nature.* 374:163–165.
41. Rathmell, J.C., M.P. Cooke, W.Y. Ho, J. Grein, S.E. Townsend, M.M. Davis, and C.C. Goodnow. 1995. CD95 (Fas)-dependent elimination of self-reactive B cells upon interaction with CD4+ T cells. *Nature.* 376:181–184.
42. Radic, M.Z., J. Mackle, J. Erikson, C. Mol, W.F. Anderson, and M. Weigert. 1993. Residues that mediate DNA binding of autoimmune antibodies. *J. Immunol.* 150:4966–4977.
43. Han, S., B. Zheng, D.G. Schatz, E. Spanopoulou, and G. Kelsoe. 1996. Neoteny in lymphocytes: Rag1 and Rag2 expression in germinal center B cells. *Science.* 274:2094–2097.
44. Hikida, M., M. Mori, T. Takai, K. Tomochika, K. Hamatani, and H. Ohmori. 1996. Reexpression of RAG-1 and RAG-2 genes in activated mature mouse B cells. *Science.* 274: 2092–2094.
45. Hiom, K., and M. Gellert. 1997. A stable RAG1-RAG2-DNA complex that is active in V(D)J cleavage. *Cell.* 88:65–72.
46. Hikida, M., M. Mori, T. Kawabata, T. Takai, and H. Ohmori. 1997. Characterization of B cells expressing recombination activating genes in germinal centers of immunized mouse lymph nodes. *J. Immunol.* 158:2509–2512.
47. Hertz, M., V. Kouskoff, T. Nakamura, and D. Nemazee. 1998. V(D)J recombinase induction in splenic B lymphocytes is inhibited by antigen-receptor signalling. *Nature.* 394:292–295.
48. Huse, W.D., L. Sastry, S.A. Iverson, A.S. Kang, M. Alting Mees, D.R. Burton, S.J. Benkovic, and R.A. Lerner. 1989. Generation of a large combinatorial library of the immunoglobulin repertoire in phage lambda. *Science.* 246:1275–1281.